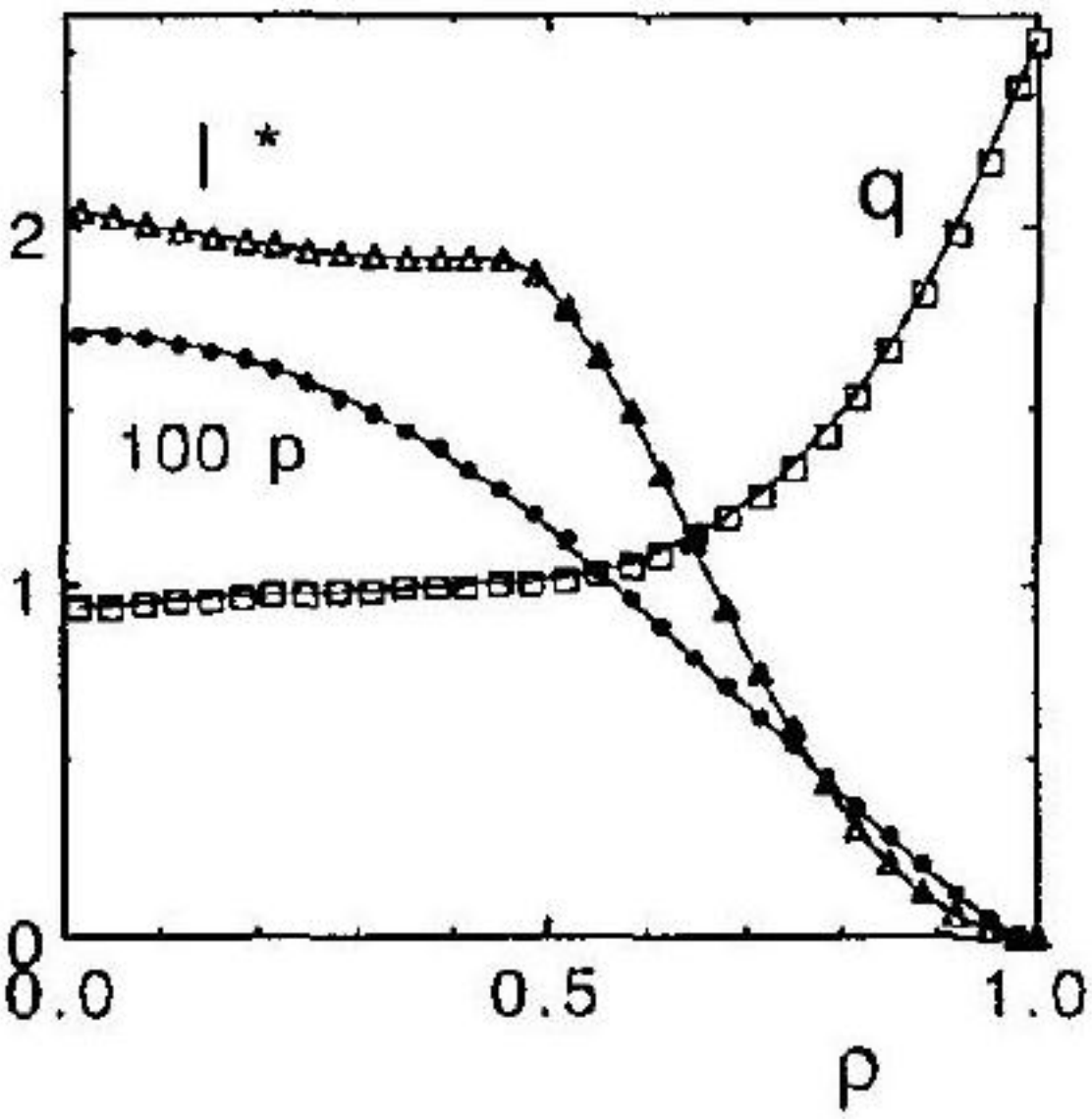

Figure 1: *Radial profiles for pressure, surface averaged toroidal current density, and safety factor for standard equilibrium with* $\beta_p = 0.4$.

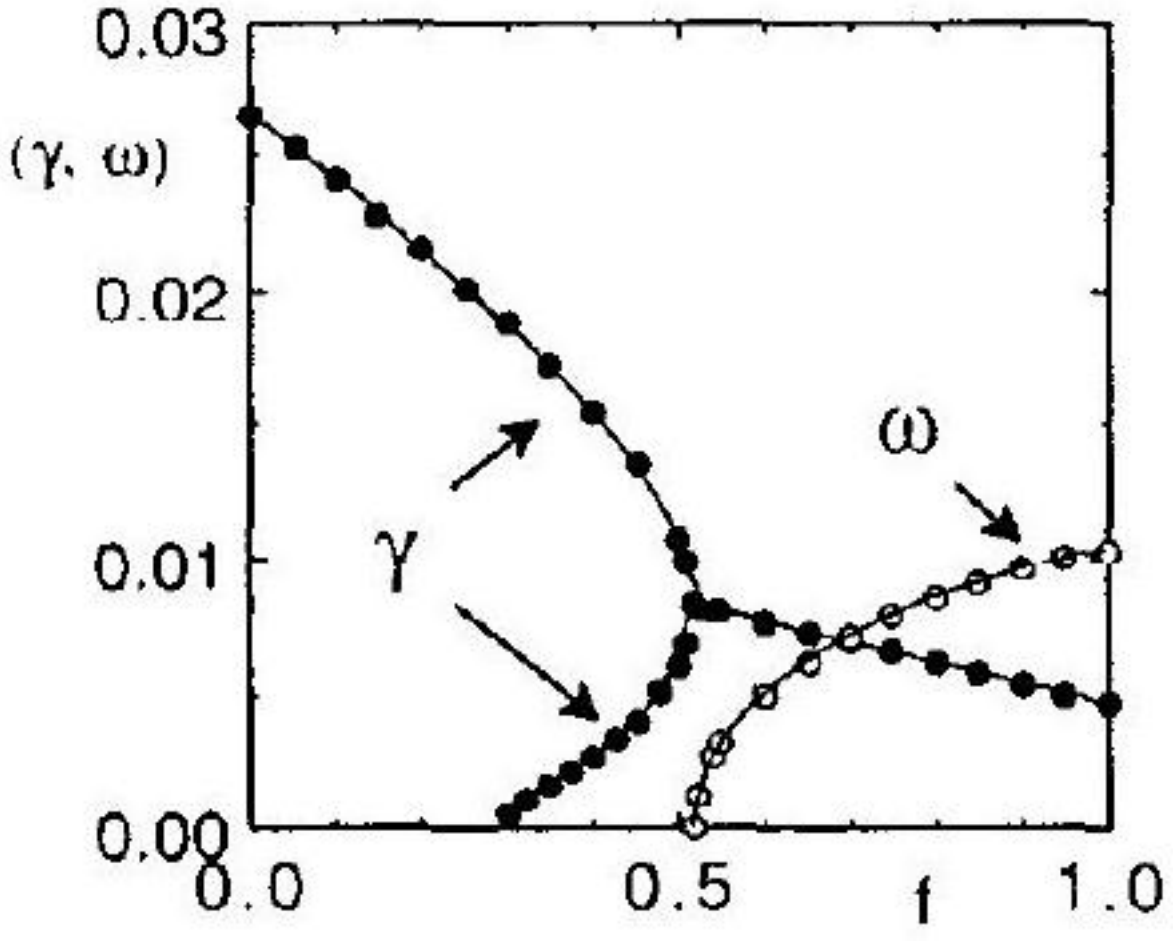

Figure 2: *Growth rate γ and frequency ω versus the trapped particle multiplier f for the standard case $\beta_p = 0.4$ and $T_e = T_i$ and the electrostatic potential turned off. Note the second branch that does not connect to the MHD mode at $f = 0$, coalescence, and the formation of a complex conjugate pair.*

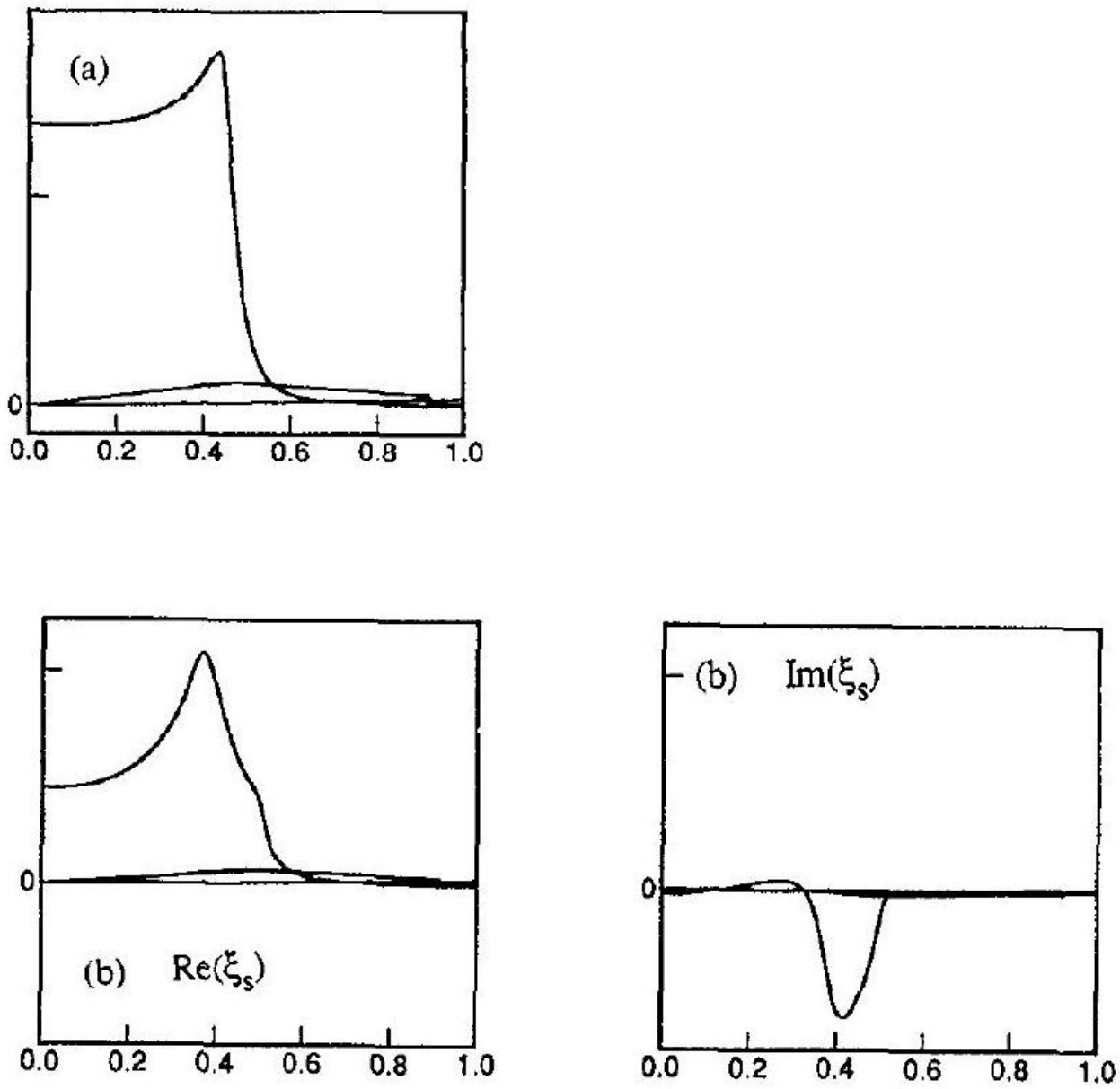

Figure 3: *Fourier components of the normal displacement for two cases in Fig. 2. (a) Second (i.e., non-MHD) branch at* $f = 0.35$ *with* $\gamma = 1.7 \times 10^{-3}\omega_A$. *(b) Rotating branch at* $f = 1$ *with* $\gamma = 5.1 \times 10^{-3}\omega_A$, $\omega = 9.8 \times 10^{-3}\omega_A$.

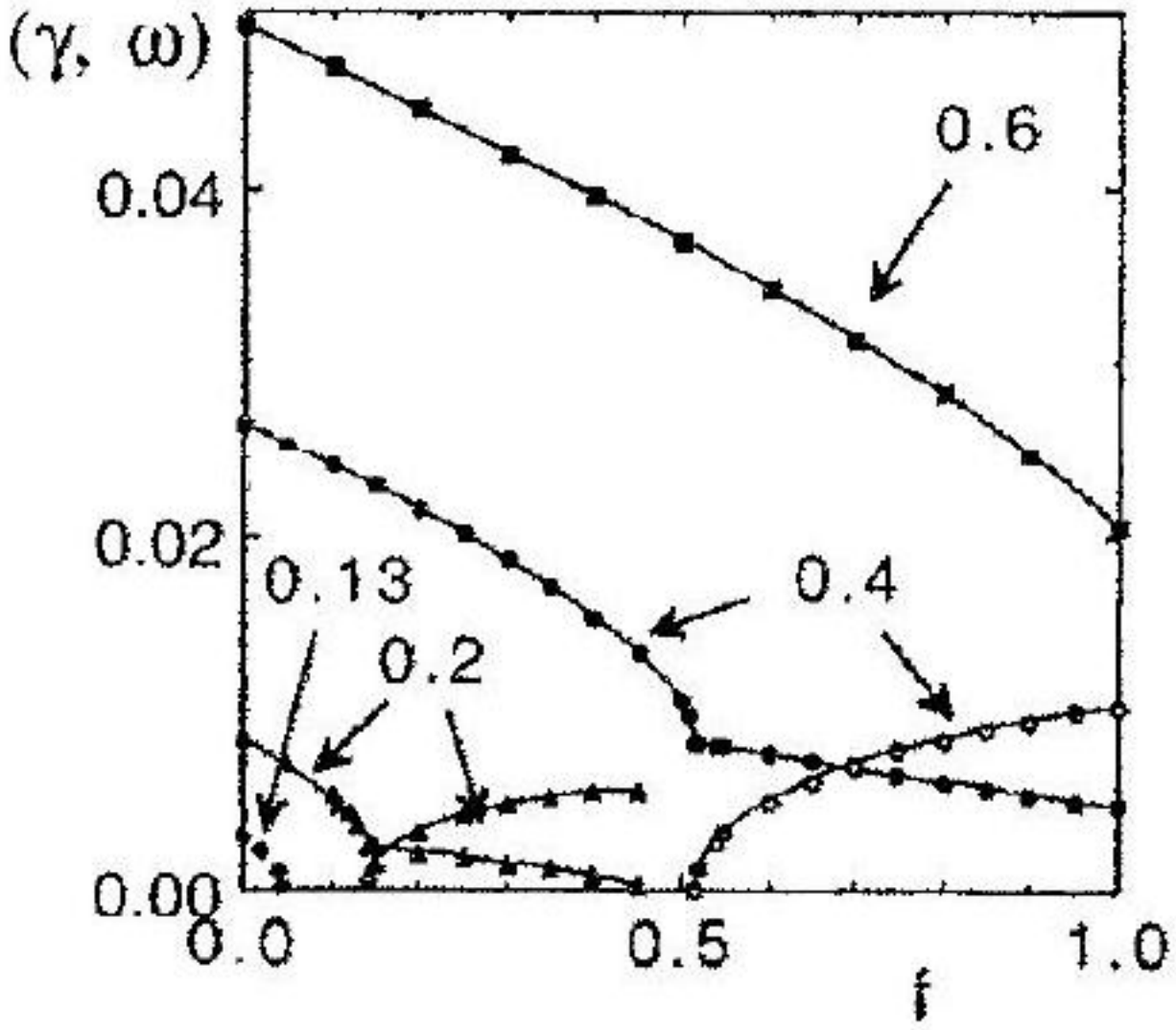

Figure 4: *Eigenvalues vs trapped particle multiplier for different idealMHD driving energies. Solid symbols give growth rates and open symbols frequencies. The curves are labeled by* β_p *at the* $q = 1$ *surfacc.*

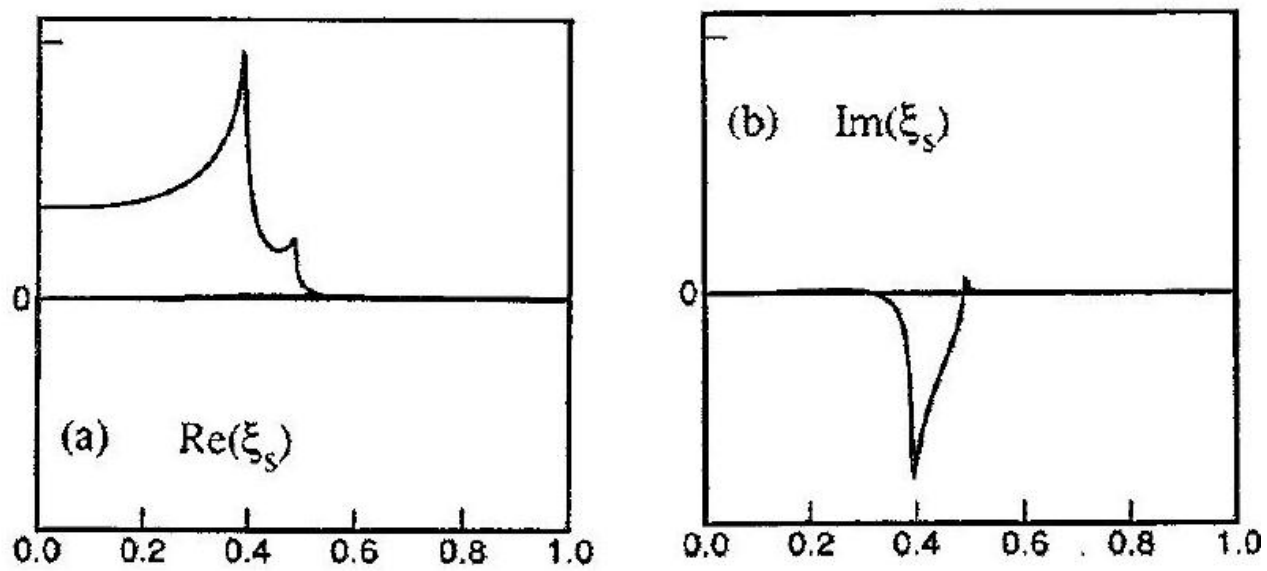

Figure 5: *Fourier components of normal displacement ξ_s close to marginal stability at $\beta_p = 0.2, f = 0.47$ with eigenvalue $\gamma = 0.3 \times 10^{-3}\omega_A$, $\omega = 5.7 \times 10^{-3}\omega_A$. Note that ξ_s approaches a logarithmically singular behavior at $q = 1 \pm \omega/\omega_A$ as $\gamma \to 0$. (a) gives the real and (b) the imaginary part of ξ_s.*

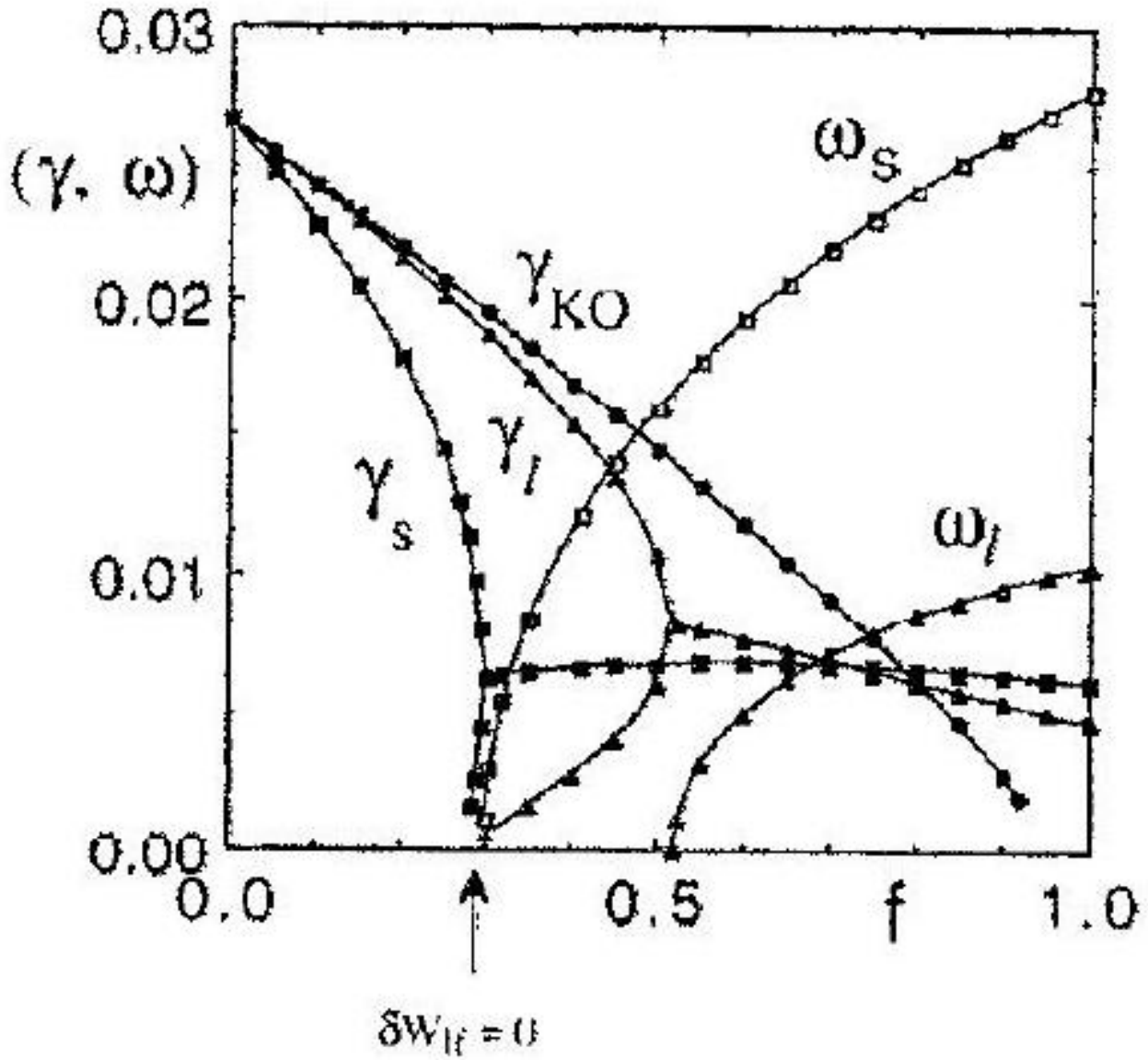

Figure 6: *Bifurcation dingram for different* ω_*/ω_A *(or different machine size) and the same equilibrium as in Fig. 2 with* $\beta_p = 0.4$ *and* $T_e = T_i$*. Subscripts on frequencies and growth rates indicate: s-"small", and L-"large" tokamak parameters, and KO-Kruskal-Oberman, or infnitely large tokamak. Note that drift effects are stabilizing when the mode rotation is slow* $(f < 0.7)$ *but becomes destabilizing for faster rotation* $(f > 0.85)$.

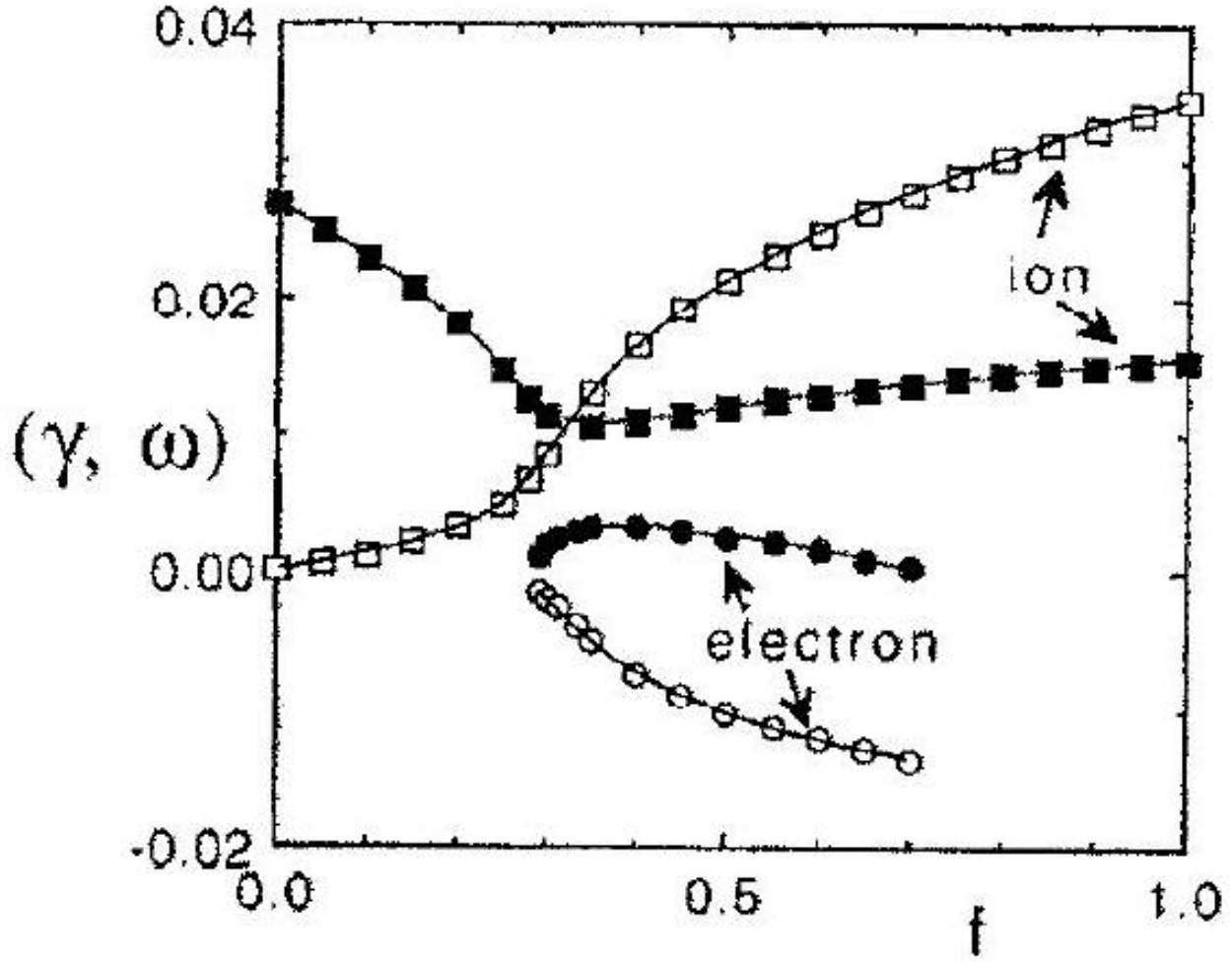

Figure 7: *Asymmetric bifurcation diagram for unequal temperatures $T_i/T_e = 3$ and $\beta_p = 0.4$. Filled symbols show growth rates and open symbols rotation frequencies. The mode rotating in the direction of the hotter species is destabilized by the drift resonance.*

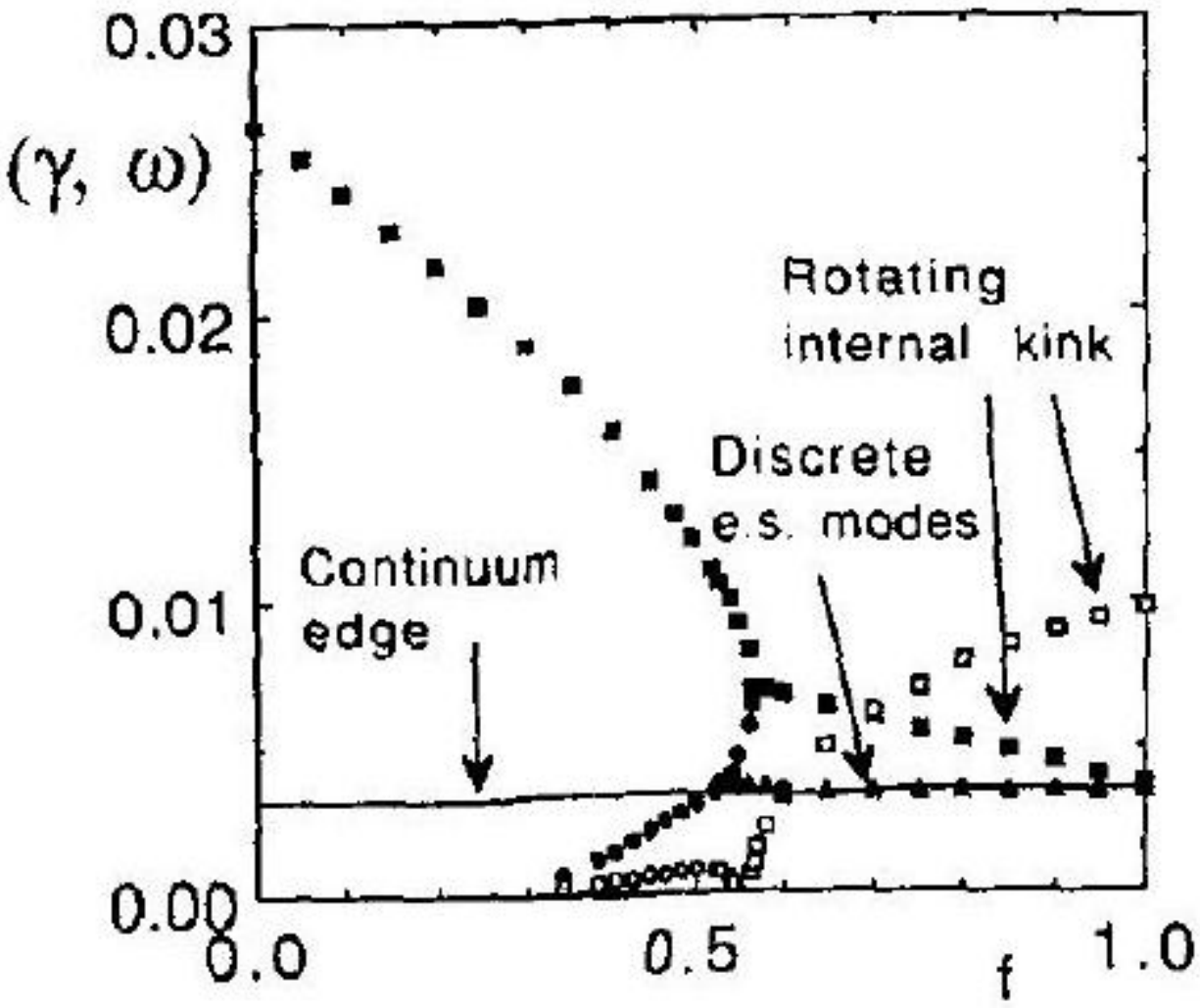

Figure 8: *Frequencies and growth rates versus trapped particle multiplier with electrostatic perturbations included. Growth rates are indicated by solid and frequencies by open symbols. The line marked continuum edge shows that maximum growth rate of the continuum of electrostatic trapped particle modes.*

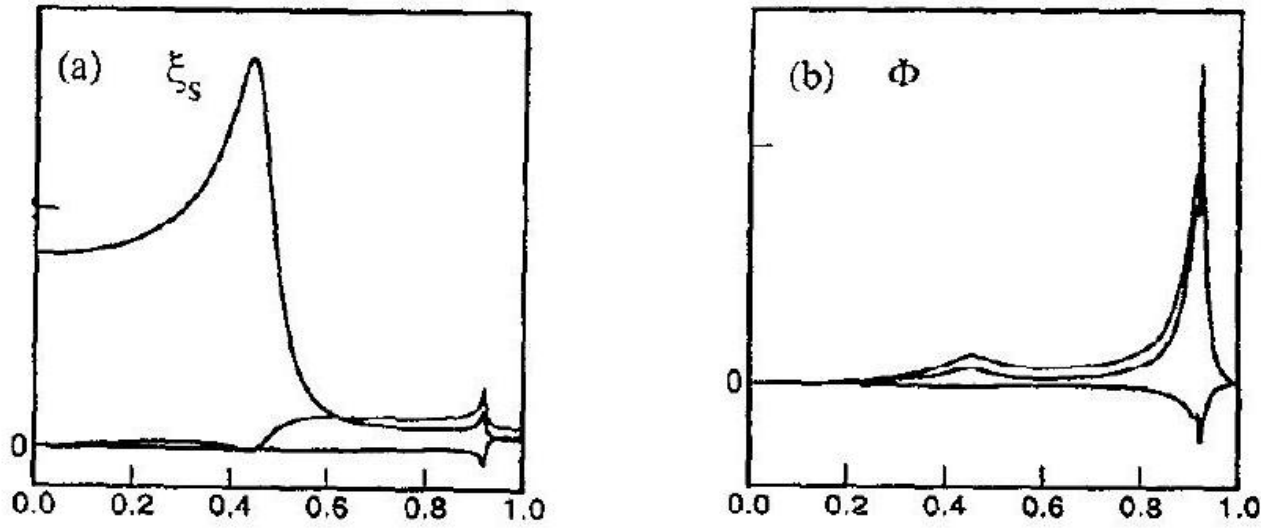

Figure 9: *Mode structure of (a) the normal displacement ξ_s and (b) the electrostatic potential Φ for a discrete coupled trapped particle-internal kink mode at $\beta_p = 0.4, f = 1$. The mode growth rate, $\gamma = 3.6 \times 10^{-3}\omega_A$, is just above the electrostatic continuum.*

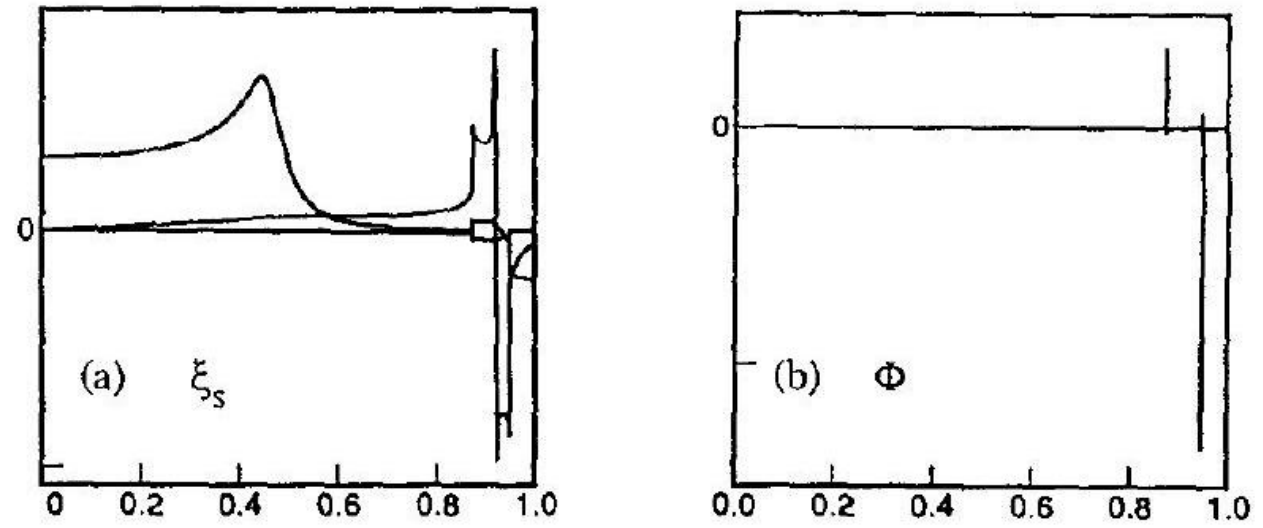

Figure 10: *Mode structure of (a) the normal displacement ξ_s and (b) the electrostatic potential Φ for a singular, coupled trapped particle-internal kink mode at $\beta_p = 0.4, f = 1$. The growth rate, $\gamma = 3.2 \times 10^{-3}\omega_A$, lies within the electrostatic continuum. Note the two sharp spikes in Φ at the two radii where the local dispersion relation is satisfied.*

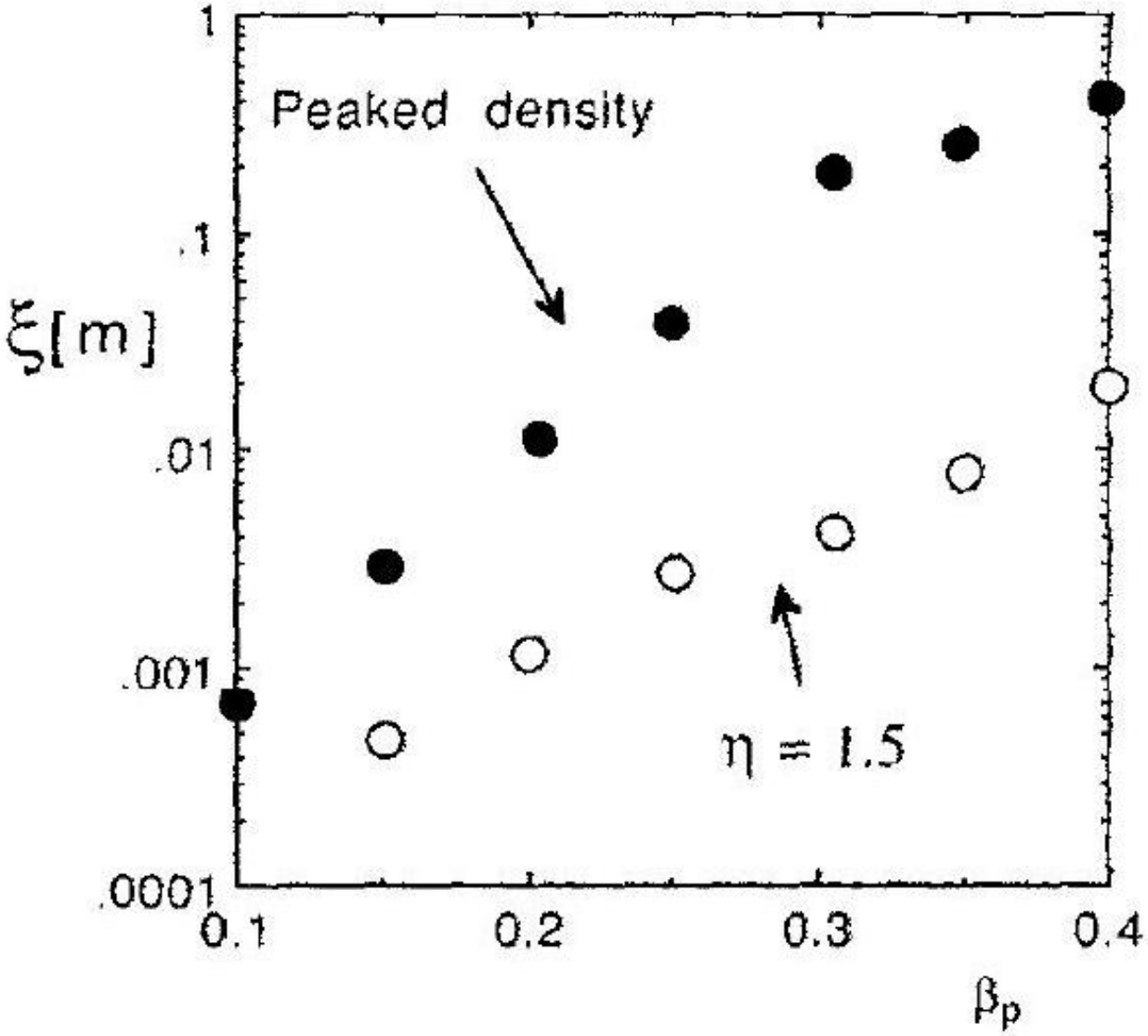

Figure 11: *Central displacement caused by a saturated trapped particle mode for two different density profiles. Note the dramatic increase in displacement with pressure.*

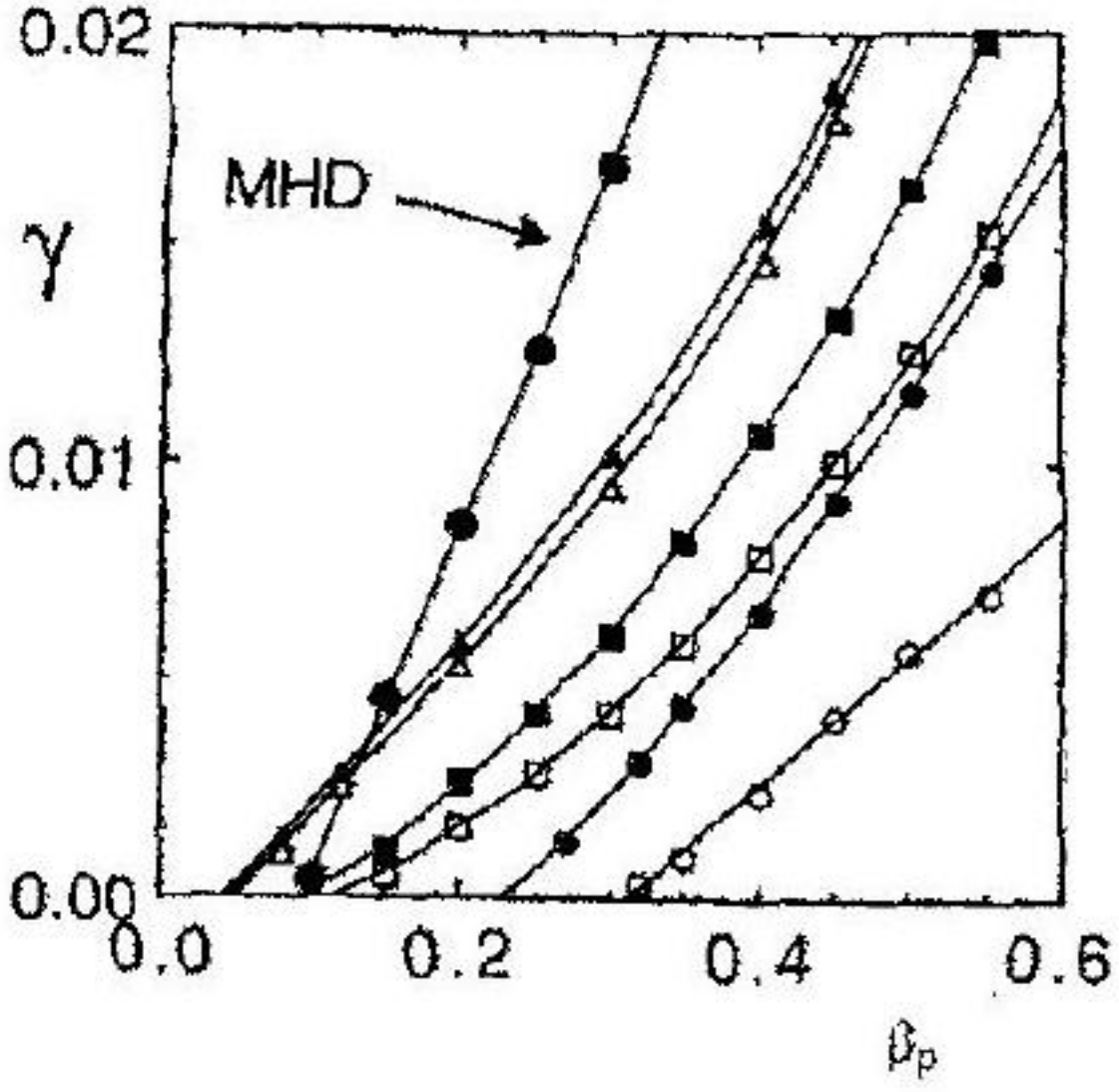

Figure 12: *Growth rates of the electromagnetic mode versus β_p for small tokamak parameters and different assumptions. The MHD result is identified by an arrow and the drift kinetic results are identified as follows: filled symbols give the nonelectrostatic results (Φ turned off), open symbols show results with Φ included, circles represent $T_i/T_e = 1$, squares: $T_i/T_e = 1.5$, and triangles: $T_i/T_e = 3$.*